Identification of the Preferential-Bonding Effect of Disubstituted Alkane Derivatives Using Scanning Tunneling Microscopy

Sai-Long Xu, Shu-Xia Yin, Han-Pu Liang, Chen Wang,* Li-Jun Wan,* and Chun-Li Bai*

Institute of Chemistry, the Chinese Academy of Sciences, Beijing100080, China

Received: May 22, 2003; In Final Form: August 8, 2003

The characteristics of the assembling behavior of three disubstituted alkane derivatives, 1,16-hexadecanediol ($HO(CH_2)_{16}OH$), 1,18-octadecanedionic acid ($HOOC(CH_2)_{18}COOH$), and 16-hydroxyhexadecanoic acid ($HO(CH_2)_{15}COOH$) have been investigated by use of scanning tunneling microscopy (STM). Three different kinds of supramolecular structures on graphite surfaces are observed, suggesting that intermolecular hydrogen bonding between two carboxyl groups of $HO(CH_2)_{15}COOH$ molecules is the preferential one among carboxyl and hydroxyl groups. The preference is also confirmed by the self-assembled structures of 16-mercaptohexadecanoic acid and the coadsorptions of $HO(CH_2)_{16}OH$ with *p*-phthalic acid (PA) and $HO(CH_2)_{15}COOH$ with PA. Theoretical simulation results on these systems support the STM observations.

Introduction

Self-assembled monolayers of organic molecules on a solid substrate surface have been of particular interest in the past decade.[1−12] With the aid of scanning tunneling microscopy (STM) and many other surface characterization techniques, a rich variety of ordered two-dimensional (2D) monolayers of monosubstituted alkane derivatives have been observed. The molecular arrays are governed by various soft bonds,[4] from primarily van der Waals interaction (such as the case for simple alkanes)[8] and hydrogen bonds (such as alcohols and acids)[3,9] to electrostatic interaction (such as cationic surfactants)[11] and dipolar interaction (such as aldehydes).[12] As one of the most useful interactions, hydrogen bonding is widely used and studied in molecular self-assembly. It is well-known from earlier STM studies that *n*-alkanes, organized by van der Waals forces, are packed into a straight lamella with a 90° angle between the molecular axis and the directions of lamellae.[2] For monosubstituted *n*-alkane derivatives, such as thiols, amines, and alcohols, head-to-head connection through hydrogen bonding is commonly formed, showing a 60° angle between the molecular axis and the directions of lamellae.[2,13,14] When two or more functional groups are involved, such as with disubstituted alkane derivatives, these functional groups can induce the formation of supramolecular self-assembly. For example, 1,2-dihydroxyoctadencane forms a lamella-type structure with a 65° angle of alkyl chains relative to the lamella,[15] whereas 1,14-tetradecanediol forms a supramolecular arrangement with a herringbone angle of 120° between alkyl chains.[16] 16-Hydroxyhexadecanoic acid ($HO(CH_2)_{15}COOH$) and 15-hydroxypentadecanoic acid[3] self-assemble into the network through multiple hydrogen bonding showing the "odd−even" effect. These observations indicate that the molecular packing arrangements are influenced by the competitive and collaborative interactions between these different functional groups. It is of genuine interest to understand the interactions of functional groups (especially hydrogen bonding) for clarifying the supramolecular structures.

In the present paper we study the effect of double functional groups on the supramolecular structures and particularly the hydrogen bonding between the different substituted groups involving $HO(CH_2)_{15}COOH$ which has also been studied in a recent work.[3] In addition, by using *p*-phthalic acid (PA) as a "chemical marker" which displays enhanced contrast in the STM images, the self-assembled structures of 16-mercaptohexadecanoic acid, 16-hydroxyhexadecanoic acid coadsorbed with *p*-phthalic acid, and 1,16-hexadecanediol coadsorbed with *p*-phthalic acid are also observed. The results are consistent with the preferential hydrogen-bonding mechanism. Molecular mechanics simulations and density functional calculations provided supportive evidence to the analysis of functional group interactions and the monolayer structures.

Experimental Section

1,16-Hexadecandiol $HO(CH_2)_{16}OH$ (Fluka, ≥98%), 16-hydroxyhexadecanoic acid $HO(CH_2)_{15}COOH$ (Aldrich, ≥98%), 1,18-octadecanedionic acid $HOOC(CH_2)_{18}COOH$ (TCI, ≥98%), and 16-mercaptohexadecanoic acid $HS(CH_2)_{15}COOH$ (Aldrich, ≥98%) were used as received without further purification and dissolved in mixed toluene/ethanol solvent (8:2 v/v). The mixtures (1:1 molar ratio) of $HO(CH_2)_{16}OH$/*p*-phthalic acid PA (TCI, >99%) and $HO(CH_2)_{15}COOH$/PA were dissolved in mixed toluene/ethanol solvent (8:2 v/v), respectively. The concentrations of all the solutions were less than 1 mg/mL. All the samples were prepared by depositing a droplet (∼2 mL) of solution on a freshly cleaved surface of highly oriented pyrolytic graphite (HOPG) (quality ZYB, Digital Instruments, Santa Barbara, CA). The solvents were completely evaporated prior to STM studies.

STM characterizations were performed on a Nanoscope IIIa SPM (Digital Instruments, Santa Barbara, CA) under ambient conditions. The STM tips were mechanically formed Pt/Ir wire (90/10). All STM images were recorded using the constant current mode. The specific tunneling conditions are given in the figure captions. The STM images were recorded at both positive and negative sample bias without any appreciable contrast variations. Only the images taken at positive bias are presented in this work.

* Corresponding authors. Phone/Fax: +86-10-62558934. E-mail: wangch@iccas.ac.cn (C.W.); clbai@iccas.ac.cn (C.L.B.); wanlijun@iccas.ac.cn (L.J.W.).

10.1021/jp035425x CCC: $27.50
Published on Web 12/13/2003

Density functional calculations (DFT) and molecular mechanics simulations were performed to explore the interactions of the functional groups and the self-assembled monolayer, respectively. The DFT computations were carried out using Gaussian 94[17] software and molecular mechanics simulations were performed using Materials Studio software.[18]

Results and Discussions

Under ambient conditions the structural details of self-assembled monolayers for three disubstituted molecules HO-$(CH_2)_{16}$OH, HOOC$(CH_2)_{18}$COOH, and HO$(CH_2)_{15}$COOH on graphite were acquired by STM. These three disubstituted molecules can self-assemble into 2D hydrogen-bonded networks on graphite through connections of both headgroups and end groups. This situation is different from the self-assembly of monosubstituted alkane derivatives. For HO$(CH_2)_{16}$OH, herringbone lamellae are formed and extend in a zigzag manner on the graphite surface. Figure 1a shows a high-resolution STM image for the self-assembled monolayer of HO$(CH_2)_{16}$OH on graphite. It can be seen that the lamella consists of two V-type molecular rows crossing each other at a herringbone angle of 120°. The troughs at the ends of the adjacent lamellae have an average length of 0.27 ± 0.2 nm. The alkyl chains are tilted by 60° with respect to the direction of the lamellae, which is in good agreement with the previous report for HO$(CH_2)_{14}$OH.[2,14] It is known that in order to meet the requirement of H-bonding and the registry of alkyl chains to the graphite lattice, OH groups are paired together leading to a characteristic angle of 60° between the alkyl chains and the lamellae axis.[14,19] On the basis of the STM observations and molecular mechanics simulations, the molecular arrangement of HO$(CH_2)_{16}$OH on graphite is shown in Figure 1b. It can be seen that HO$(CH_2)_{16}$OH molecules form a supramolecular structure with neighboring lamellae connected to each other through hydrogen bonding OH···OH.

Figure 2a presents a high-resolution STM image of a HOOC-$(CH_2)_{18}$COOH monolayer on graphite. It can be seen that the self-assembled monolayer is characterized by straight lamellae, that is, the angle between the alkyl chains and the lamella main axis is nearly 90°. The dark troughs between the neighboring lamellae contain many dark spots, which are attributed to the location of the COOH···COOH moieties of two head-to-head HOOC$(CH_2)_{18}$COOH molecules. The head-to-head arrangement of molecules in neighboring lamellae is accompanied by an offset of half a molecule width similar to the assemblies of stearic acid[9,20] in order to satisfy the hydrogen-bonding requirements. A supramolecular network of HOOC$(CH_2)_{18}$COOH molecules is presented in Figure 2b, in which two HOOC-$(CH_2)_{18}$COOH molecules are paired together to form a dimer through two single hydrogen bonds of COOH groups.

Noticeably, the packing structure for the self-assembled monolayer of HO$(CH_2)_{15}$COOH exhibits the combined characteristics of HO$(CH_2)_{16}$OH and HOOC$(CH_2)_{18}$COOH. Our experiments confirm the recent report that the lamella of HO-$(CH_2)_{15}$COOH is not straight but is instead tilted by an angle of 60° between the alkyl chain and the lamella direction.[3] Moreover, the head-to-head molecules in the neighboring lamellae are parallel. It has been suggested that HO$(CH_2)_{15}$-COOH molecules form a supramolecular structure through quadruple hydrogen-bonded tetramers.[3]

To help directly differentiate the assembling effect of carboxyl groups from that of other functional groups, the self-assembled monolayer of the HS$(CH_2)_{15}$COOH molecule was investigated. It is well-known from previous studies that in STM images the thiol group in alkane derivatives is characterized by bright

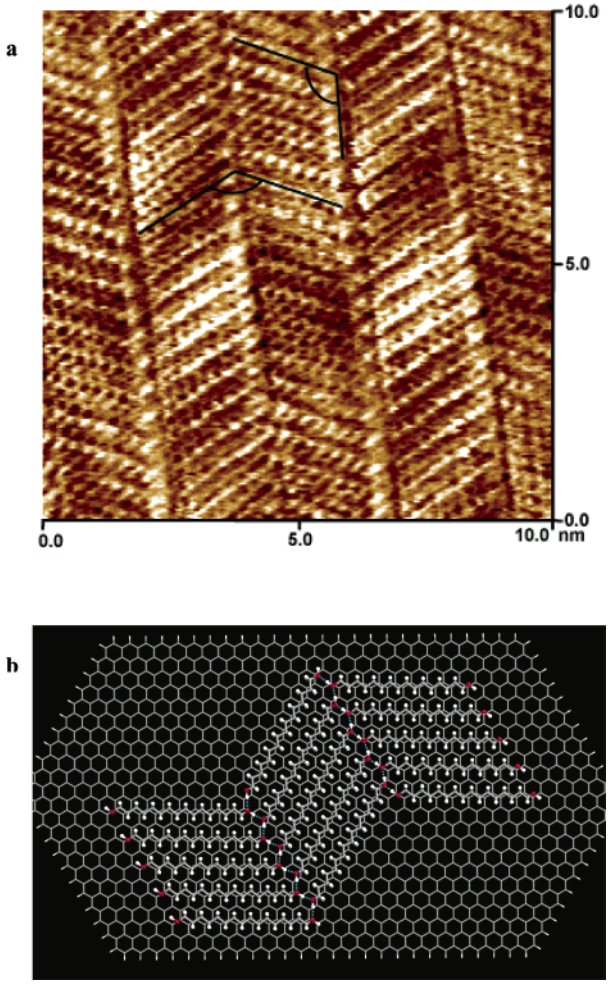

Figure 1. (a) High-resolution STM image of the 1,16-hexadecanediol (HO$(CH_2)_{16}$OH) hydrogen-bonded network on graphite. Tunneling condition: 619 mV, 1.0 nA. (b) Molecular model of the assembly deduced from the STM image.

contrast, whereas the carboxyl group function appears as a dark contrast.[14] Thus, carboxyl groups can be easily recognized from thiol groups. Figure 3a shows the high-resolution STM image of the HS$(CH_2)_{15}$COOH self-assembled structure on graphite. It can be observed that the straight lamella consists of two parallel molecular rows. The bright band indicated by the arrow is attributed to the thiol groups. The dark trough corresponds to the COOH group, which does not adopt the interdigitated alignment, in contrast to monosubstituted acids and HO$(CH_2)_{15}$-COOH. The HS$(CH_2)_{15}$COOH molecules are packed parallel between the straight lamellae, clearly indicating the effect of the COOH group on the molecular arrangement. Interestingly, in all the repeated STM experiments no arrangement of a carboxyl group adjacent to a thiol group has been obtained. This implies that HS$(CH_2)_{15}$COOH molecules form a hydrogen-bonded supramolecular structure exclusively through COOH···COOH and SH···SH interactions. The molecular model for HS$(CH_2)_{15}$COOH is given in Figure 3b. The double hydrogen bonding of the COOH···COOH groups is the dominant driving force for the formation of the HS$(CH_2)_{15}$COOH supramolecular system on graphite. The hydrogen bond between the thiol group and the carboxyl group does not form, which is different from the assemblies of HO$(CH_2)_{15}$COOH molecules. However, in both supramolecular systems the strong COOH···COOH interaction is the preferential one in the process of self-assembly.

Furthermore, the preference of carboxyl hydrogen bonding is directly confirmed by the coadsorption of HO$(CH_2)_{15}$COOH/

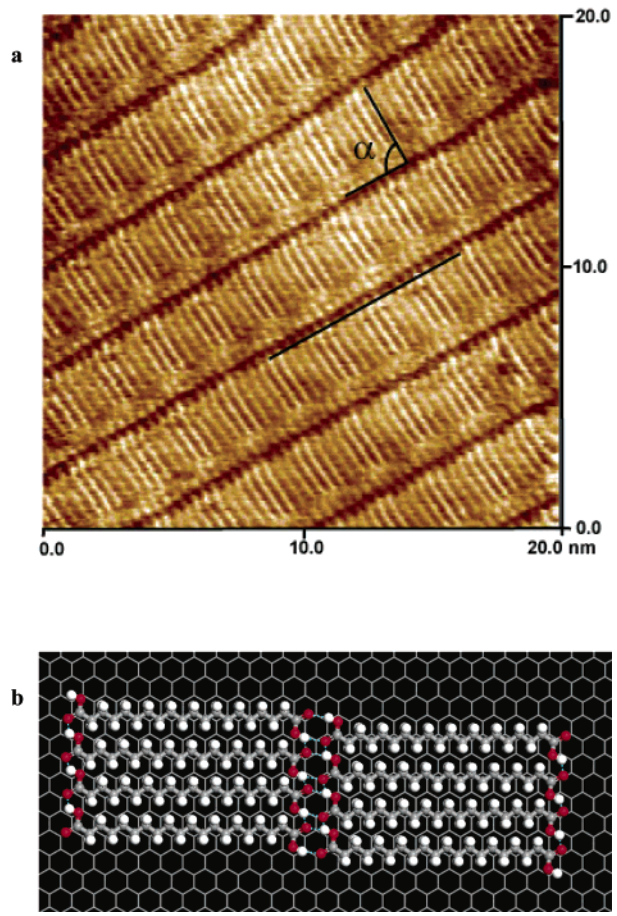

Figure 2. (a) High-resolution STM image of the 1,18-octadecanedionic acid ($HOOC(CH_2)_{18}COOH$) hydrogen-bonded network on graphite. Tunneling condition: 774 mV, 1.40 nA. (b) Molecular model of the assembly arrangement deduced from the STM image.

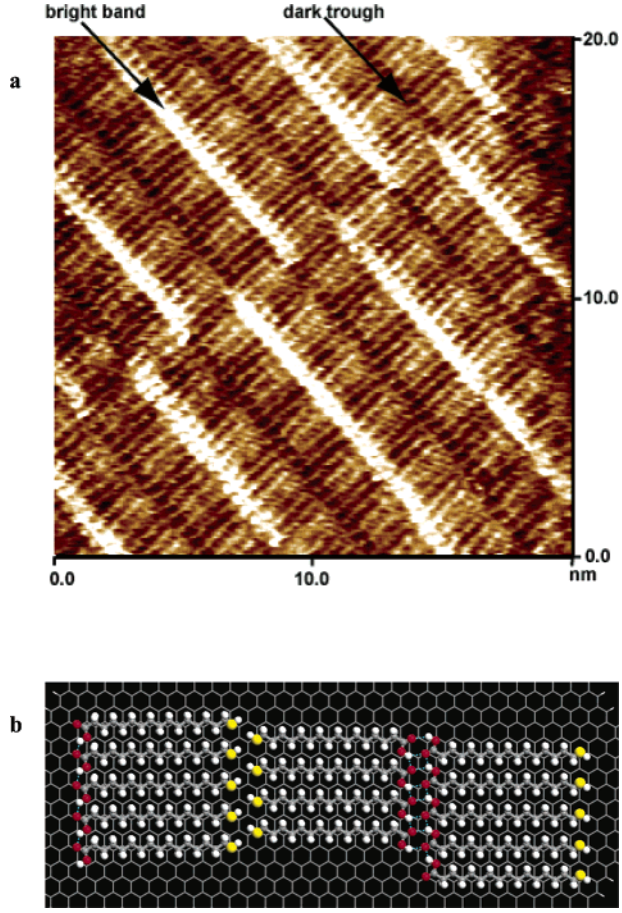

Figure 3. (a) High-resolution STM image of the 16-mercaptohexadecanoic acid $HS(CH_2)_{15}COOH$ hydrogen-bonded network on graphite. Tunneling condition: 854 mV, 920 nA. (b) Molecular model of the assembly arrangement deduced from the STM image.

PA and $HO(CH_2)_{16}OH$/PA on graphite. The self-assembled supramolecular structures are determined by the competitions between the interactions of COOH···COOH, OH···COOH, and OH···OH. Parts a and b of Figure 4 provide the detailed structures for the monolayers of $HO(CH_2)_{15}COOH$ and $HO(CH_2)_{16}OH$ coadsorbed with PA molecules on graphite, respectively. In Figure 4a, $HO(CH_2)_{15}COOH$ and PA form sandwich-like structures. The bright contrast regions and lamellae structure are attributed to PA and $HO(CH_2)_{15}COOH$ molecules, respectively. The formation of the sandwich-like supramolecular structure results from the strong interaction of the COOH··· COOH groups between both the PA and the $HO(CH_2)_{15}COOH$ molecules. In this coadsorption system, the PA molecules could actually serve as a "chemical marker" to recognize the COOH groups of $HO(CH_2)_{15}COOH$, which is similar to the case of 4,4′-bipyridine whose pyridine group could form hydrogen bonds with stearic acid molecules.[21,22] It can be seen that compared with the $HO(CH_2)_{15}COOH$ tetramer, the sandwich-like structures maximize the surface coverage and minimize the surface free energy.

On the other hand, for the coadsorption of $HO(CH_2)_{16}OH$ with PA shown in Figure 4b, the phase separation of the $HO(CH_2)_{16}OH$ and PA molecules can be observed as two markedly different domains. This is similar to the report for the phase separation of 1-undecanol and isophthalic derivatives[23] on graphite. In the STM image, the dark and bright domains can be identified as those of $HO(CH_2)_{16}OH$ and PA, respectively. As mentioned before the domain of $HO(CH_2)_{16}OH$ is driven by the OH···OH bonds between the $HO(CH_2)_{16}OH$ molecules, whereas the domain of PA is dominated by the COOH···COOH bonds between the PA molecules. However, no self-assembled structures connected through hydrogen bonding between hydroxyl and carboxyl groups are found. In the adsorption process, COOH···COOH hydrogen bonding is preferred to the other types of hydrogen bonding, and the OH···O═C hydrogen bond cannot be formed when $HO(CH_2)_{15}COOH$ and PA or $HO(CH_2)_{16}OH$ are closely packed through COOH···COOH or OH···OH interactions.

Density functional and molecular mechanics calculations were performed to explore the interactions of the functional groups and self-assembled monolayer, respectively. Structures of dimers consisting functional groups of COOH and OH were optimized at the levels of B3LYP/6-31g and B3LYP/6-311g**. Considering the computation limits and weak van der Waals interactions between alkyl chains, monosubstituted C_2H_5COOH and $C_2H_5CH_2OH$ were used as the models for studying the interactions of the functional groups.

Figure 5 illustrates the structures of the dimers linked via hydrogen bonds optimized at the level of B3LYP/6-311g**. It is shown that the dimer of C_2H_5COOH contains two linear hydrogen bonds, OH···O═C, with the molecules coplanar and the ethyl groups extending to opposite sides. The distances of these two hydrogen bonds are the same (1.67 Å). For the complex of $C_2H_5CH_2OH···C_2H_5COOH$ there are also two hydrogen bonds which are nonlinear with deviations of 42° and 22°, respectively. The OH···O═C distance is 1.96 Å and the OH···OH distance is 1.76 Å. In the $C_2H_5CH_2OH···C_2H_5CH_2OH$ dimer the minimum was obtained which contains a linear

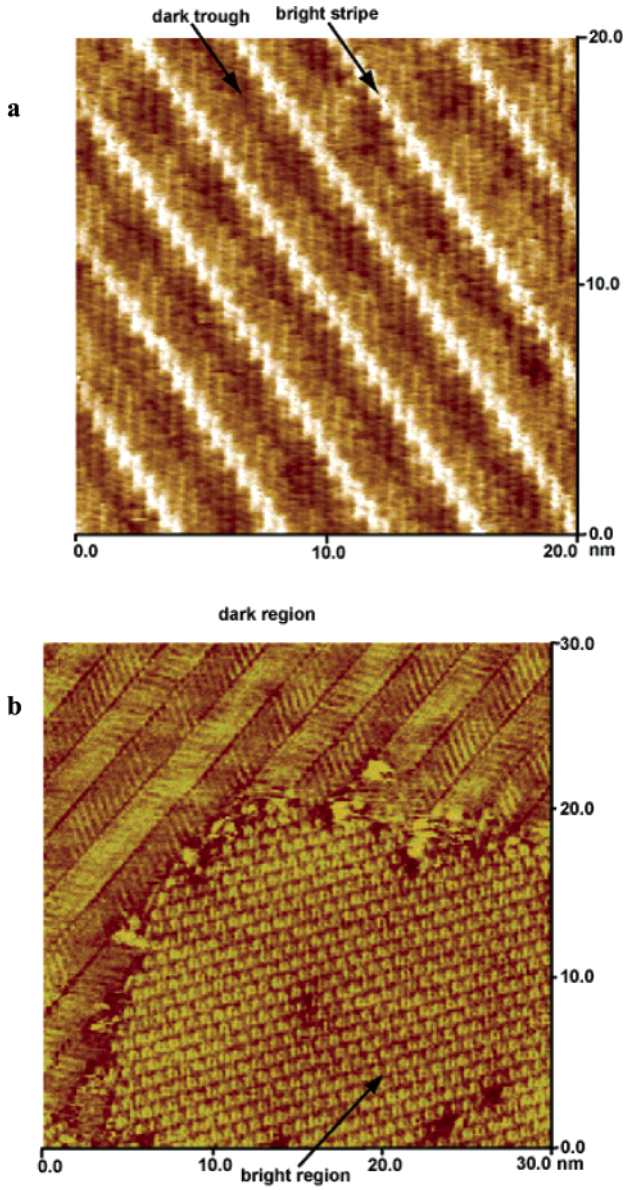

Figure 4. (a) STM image of the $HO(CH_2)_{15}COOH$ coadsorbed with *p*-phthalic acid (PA) modular structure on graphite. Tunneling condition: 840 mv, 1.12 nA. (b) STM image of the phase-separated domains of 1,16-hexadecanediol ($HO(CH_2)_{16}OH$) and PA on graphite. Tunneling condition: 832 mV, 965 nA.

hydrogen bond with a distance of 1.88 Å. It is apparent that the hydrogen bonds in the $C_2H_5CH_2OH\cdots C_2H_5COOH$ complex show the features of OH···O═C and OH···OH but are relatively stronger than OH···OH and weaker than OH···O═C, respectively. The interaction energies for these structures show similar trends. For $C_2H_5CH_2OH\cdots C_2H_5COOH$ the interaction energy with counterpoise correction for the basis set superposition error (BSSE) is −9.26 kcal/mol, which is smaller than that of the $C_2H_5COOH\cdots C_2H_5COOH$ dimer and larger than that of the $C_2H_5CH_2OH\cdots C_2H_5CH_2OH$ dimer. This proves that the interaction of functional groups decreases in the order COOH··· COOH, COOH···OH, and OH···OH. This trend is also consistent with the above STM observations.

The monolayers for three disubstituted species $HO(CH_2)_{16}$-OH, $HOOC(CH_2)_{18}COOH$, and $HO(CH_2)_{15}COOH$ were simulated using the molecular mechanics method and the consistent valence force field (CVFF) by Materials Studio[18] software. For the former two species, supramolecular structures are obtained which are connected through hydrogen bond networks and all

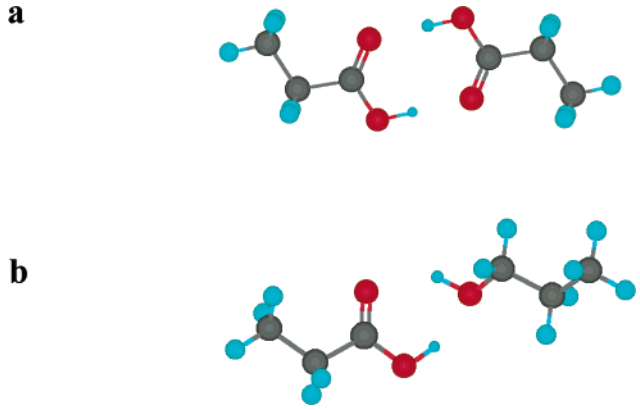

Figure 5. Structures of hydrogen-bonded dimers optimized at the level of B3LYP/6-311g**: (a) $C_2H_5COOH\cdots C_2H_5COOH$; (b) $C_2H_5COOH\cdots C_2H_5CH_2OH$.

alkyl in commensuration with the graphite surface similar to the those of the monosubstituted alcohol and carboxylic acid. So herein we mainly focus on the results of $HO(CH_2)_{15}COOH$. In the molecular mechanics simulations on the monolayer of $HO(CH_2)_{15}COOH$, both the cis and trans rotamers for OH are considered to meet the hydrogen bond requirements and the registry to the underlying graphite. On the basis of the STM images and DFT calculations, the tetramer connected through the interaction of COOH···COOH (forming two linear hydrogen bonds) and the interaction of OH···COOH (forming two nonlinear hydrogen bonds) were built and optimized. The results show that the arrangement involving the cis OH rotamer is more stable than that of the trans rotamer. In the arrangement with cis OH orientation, the alkyl can be commensurate with the underlying graphite and OH can pair up with COOH to form nonlinear hydrogen bonds, whereas in the arrangement with trans OH orientation, the hydrogen bonds cannot form in order to meet the requirement of alkyl registry to graphite. Thus, the system stability is reduced as a result of the lack of hydrogen bonds. Other arrangements including that of OH connected head-to-head were also built and optimized, which proved to be relatively more unstable than the tetramer arrangements. The detailed calculations will be presented in a subsequent report.

Conclusion

Three disubstituted alkane derivatives ($HO(CH_2)_{16}OH$, $HOOC(CH_2)_{18}COOH$, and $HO(CH_2)_{15}COOH$) adsorbed on graphite have been selected to explore the interactions between functional groups through intermolecular hydrogen bonding. The different assembled structures of these molecules on the graphite surface reveal the preferential COOH···COOH interactions. The enhanced contrast in STM images of $HS(CH_2)_{15}COOH$ and PA coadsorbed with $HO(CH_2)_{15}COOH$ and $HO(CH_2)_{16}OH$ provide supportive evidence for the preferential interactions.

Acknowledgment. This work is supported by the National Natural Science Foundation of China (Grants 200253 and 29825106), the National Key Project on Basic Research (Grant G 2000077501), and the Chinese Academy of Science.

References and Notes

(1) Smith, D. P. E.; Horber, H.; Gerber, C.; Binnig, G. *Science* **1989**, *245*, 43.

(2) Claypool, C. L.; Faglioni, F.; Goddard, W. A., III; Gray, H. B.; Lewis, N. S.; Marcus, R. A. *J. Phys. Chem. B* **1997**, *101*, 5978.

(3) Wintgens, D.; Yablon, D. G.; Flynn, G. W. *J. Phys. Chem. B* **2003**, *107*, 173.

(4) Griessl, S.; Lackinger, M.; Edelwirth, M.; Hietschold, M.; Heckl, W. M. *Single Mol.* **2002**, *3*, 25.

(5) Hoeppener, S.; Chi, L.; Fuchs, H. *ChemPhysChem* **2003**, *4*, 494.

(6) Cai, Y.; Bernasek, S. L. *J. Am. Chem. Soc.* **2003**, *125*, 1655.

(7) De Feyter, S.; Gesquiere, A.; Adel-Mottaleb, M. M.; Grim, P. C. M.; De Schryver, F. C.; Meiners, C.; Sieffert, M.; Valiyaveettil, S.; Mullen, K. *Acc. Chem. Res.* **2000**, *33*, 520.

(8) Rabe, J. P.; Buchholtz, S. *Science* **1991**, *253*, 424.

(9) Hibino, M.; Sumi, A.; Tsuchiya, H.; Hatta, I. *J. Phys. Chem. B* **1998**, *102*, 4544.

(10) Charra, F.; Cousty, J. *Phys. Rev. Lett.* **1998**, *80* (8), 1682.

(11) Xu, S. L.; Wang, C.; Zeng, Q. D.; Wu, P.; Wang, Z. G.; Yan, H. K.; Bai, C. L. *Langmuir* **2002**, *18*, 657.

(12) Xu, S. L.; Zeng, Q. D.; Wu, P.; Qiao, Y. H.; Wang, C.; Bai, C. L. *Appl. Phys. A* **2003**, *76*, 209.

(13) Xu, Q. M.; Wan, L. J.; Bai, C. L. *Surf. Interface Anal.* **2001**, *32*, 256.

(14) Cyr, D. M.; Venkataraman, B.; Flynn, G. W.; Black, A.; Whitesides, G. M *J. Phys. Chem.* **1996**, *100*, 13747.

(15) Qian, P.; Nanjo, H.; Yokoyama, T.; Suzuki, T. M. *Chem. Lett.* **1998**, 1133.

(16) Elbel, N.; Roth, W.; Günther, E.; von Seggern, H. *Surf. Sci.* **1994**, *303*, 424.

(17) Frisch, M. J.; Trucks, G. W.; Schlegel, H. B.; Gill, P. M. W.; Johnson, B. G.; Robb, M. A.; Cheeseman, J. R.; Keith, T.; Petersson, G. A.; Montgomery, J. A.; Raghavachari, K.; Al-Laham, M. A.; Zakrzewski, V. G.; Ortiz, J. V.; Foresman, J. B.; Cioslowski, J.; Stefanov, B. B.; Nanayakkara, A.; Challacombe, M.; Peng, C. Y.; Ayala, P. Y.; Chen, W.; Wong, M. W.; Andres, J. L.; Replogle, E. S.; Gomperts, R.; Martin, R. L.; Fox, D. J.; Binkley, J. S.; Defrees, D. J.; Baker, J.; Stewart, J. P.; Head-Gordon, M.; Gonzalez, C.; Pople, J. A. *Gaussian 94*; Gaussian, Inc.: Pittsburgh, PA, 1995.

(18) *Materials Studio*, version 2.0; Accelrys Inc., 2001.

(19) Yin, S. X.; Wang, C.; Xu, Q. M.; Lei, S. B.; Wan, L. J.; Bai, C. L. *Chem. Phys. Lett.* **2001**, *348*, 321.

(20) Yablon, D. G.; Wintgens, D.; Flynn, G. W. *J. Phys. Chem. B* **2002**, *106*, 5470.

(21) Qian, P.; Nanjo, H.; Yokoyama, T.; Suzuki, T. M. *Chem. Coummun.* **1999**, 1197.

(22) Xu, B.; Yin, S.; Wang, C.; Zeng, Q.; Qiu, X., Bai, C. *Surf. Interface Anal.* **2001**, *32*, 245.

(23) Vanoppen, P.; Grim, P. C. M.; Rücker, M.; De Feyter, S.; Moessner, G.; Valiyaveettil, S.; Müllen, K.; De Schryver. F. C. *J. Phys. Chem.* **1996**, *100*, 19636.